

TECH NOTE NO: 33
TITLE: Fracture Behavior of Functionally Graded Concrete Materials (FGCM) for Rigid Pavements
AUTHORS: Professors. J. Roesler and G. Paulino, C. Gaedicke, A. Bordelon, K. Park
Ph: (217) 265-0218, Email: jroesler@uiuc.edu
CONTACT: University of Illinois, Dept of Civil & Environmental Engineering
1211 NCEL, MC-250, Urbana, IL 61801
DATE/REV: 12/07/2006

EXECUTIVE SUMMARY

Currently in concrete pavements, a single concrete mixture design and structural surface layer are selected to resist mechanical loading without attempting to adversely affect the concrete pavement shrinkage, ride quality, or noise attenuation. An alternative approach is to design sub-layers within the concrete pavement surface which have specific functions thus achieving higher performance at a lower cost. The objective of this research was to address the structural benefits of functionally graded concrete materials (FGCM) for rigid pavements by testing and modeling the fracture behavior of different combinations of layered plain and synthetic fiber reinforced concrete materials. The three point bending beam test was used to obtain the softening behavior and fracture parameters of each FGCM. The peak loads and initial fracture energy between the plain, fiber reinforced, and functionally graded concrete material were similar signifying similar crack initiation. The total fracture energy clearly indicated the improvements in fracture behavior of FGCM relative to full-depth plain concrete. The fracture behavior of FGCM depended on the position of the fiber reinforced layer relative to the starter notch. The fracture parameters of both fiber reinforced and plain concrete were embedded into a finite element-based cohesive zone model. The model successfully captured the experimental behavior of the FGCMs and now can be implemented to predict the fracture behavior of proposed FGCM configurations and structures such as rigid pavements. This integrated approach (testing and modeling) is very promising and demonstrates the viability of FGCM for designing layered concrete pavements system.

INTRODUCTION

Rigid pavement systems are constructed at airports, in high volume traffic corridors such as interstate, highways, and arterials, ports, local streets, and parking lots. The concrete material and rigid pavement structure must be designed to be multi-functional in order to resist mechanical loadings, resist stresses from thermal and moisture gradients, survive early-age and long-term volumetric changes, attenuate noise and provide a skid, wear resistant and drainable surface layer. Currently, a single, monolithic concrete mixture design and structural surface layer is selected that attempts to optimize the aforementioned objectives by balancing the trade-offs between strength, volumetric stability, and desired surface characteristics. This standard method results in greater slab depths and may not meet all the performance criteria desired for the design.

The research, design, and manufacturing of functionally graded materials (FGM) have been extensively applied to high performance materials such as graded metals and composite metals/ceramics for high-tech applications (1-3). The concept of FGMs consists of producing steady transitions in material microstructure and composition to meet the functional requirements of an engineered component and thus enhance the overall performance of the system (3, 4). An innovative approach that can maximize the performance while minimizing the cost of the concrete pavement is to use layers with different properties at specified depths. By having continuous layers in the concrete pavement, the performance criteria of each layer can be maximized by including them only in the necessary location with the appropriate thickness.

There is an increasing performance demand placed on the materials used to construct, repair, and maintain the pavement infrastructure. However, the availability of high quality construction materials is diminishing resulting in utilization of lower quality construction and recycled materials. To make use of such materials, a multi-functional and functionally layered (or graded) concrete pavement structure could be constructed to address the multi-objective performance requirements. For example, discrete fibers could be volumetrically graded through the slab depth to improve the fatigue and fracture resistant properties in the tensile loading region of the slab. A different fiber type and volume and larger size coarse aggregate could be used in the middle or near the surface of the slab to improve the cyclic shear resistance of the concrete joints. Finally, the upper surface layer could contain concrete materials which are shrinkage and skid resistant. Potentially, this functionally graded concrete pavement system could outperform the existing homogeneous concrete material layer in terms of fatigue, strength, shrinkage, durability, and life-cycle costs.

Functionally graded concrete materials (FGCM) would be constructed in multiple layers (5) by incrementally varying the material properties. The FGCM systems could be practically constructed by modifying existing paving equipment to allow for extrusion of multi-layered concrete through a continuous feeding and auguring arrangement or in a pre-cast operation. With this method, the construction of the individual layers is completed when the concrete is still plastic, thus no discrete interfaces exist in the system.

Building layered pavements is not a new concept in the construction industry. Layered concrete paving has been used in Europe (6), was constructed in Michigan (7), and has been implemented in others areas of the United States (8). In the majority of these applications, the surface concrete mixture was designed for friction and noise while a standard concrete paving mixture was used in lower region of the slab. The primary objectives of the previous multi-layered concrete pavement systems were reduced life cycle costs and improved riding surface. Limited research was conducted to test and analyze these layered concrete pavement systems for their mechanical properties. Research on flexural strength and casting delay times have been studied for layered fiber-reinforced concrete beams (9). In addition, research on the interfacial characteristics and fatigue performance of bonded fiber-reinforced overlay systems has been studied (10).

RESEARCH OBJECTIVES AND SCOPE

The objective of this research is to explore the structural benefits of FGCM for rigid pavements by testing and simulating the fracture behavior for different combinations of layered plain and fiber reinforced concrete materials. A numerical model based on the finite element method utilizing cohesive elements with specific constitutive relations for plain and fiber reinforced concrete will be developed and its results will be compared with the experiments. By achieving these objectives, this research will demonstrate the viability of functionally graded systems and propose key concepts required for modeling and designing multi-layered concrete pavement systems.

EXPERIMENTAL PROGRAM

Testing Program

The testing program included a total of 4 specimen configurations to analyze the effect of using different combinations of concrete mixtures [plain concrete (PCC) and synthetic fibers (FRC)] on the top or bottom layer of the specimen. Three-point bending beam (TPB) specimens were utilized, as shown in Figure 1, to characterize the fracture behavior of the individual and functionally layered concrete materials. The concrete fracture parameters, derived from the TPB test, were based on the Two-Parameter Fracture Model (TPFM) (11-13) and the Hillerborg work of fracture method (14).

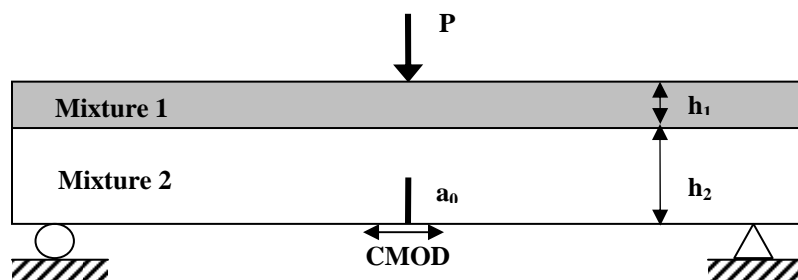


FIGURE 1. Three-point bending beam test setup for functionally layered concrete specimens.

Table 1 lists the material combinations used for the TPB testing program. The materials used for each layer are defined according to the Mixture ID in Table 2. Two beam configurations have the same concrete material in the top and bottom layer in order to characterize the fracture parameters of the individual materials. Three beam replicates were made for each material configuration.

Table 1. Experimental Testing Program.

Configuration ID	PCC/PCC	PCC/FRC	FRC/PCC	FRC/FRC
Top layer (h₁)	PCC	PCC	FRC	FRC
Bottom layer (h₂)	PCC	FRC	PCC	FRC

Mix Design and Properties

Two concrete mixtures were cast for this comparative study of FGCM: ordinary plain concrete (PCC) and fiber reinforced concrete (FRC). The mixture proportions are presented in Table 2. A crushed limestone coarse aggregate was used with a maximum aggregate size of 19 mm along with natural sand and Type I Portland cement. The FRC mixture incorporated a structural synthetic fiber at a dosage of 0.78 percent by volume, which is equivalent to 7.2 kg/m³ (12.1 lb/yd³). This fiber content was chosen since it would be the maximum feasible amount practically used by engineers in the field. Table 3 shows the properties of the synthetic fiber.

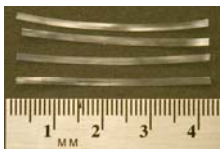
TABLE 2. Concrete Mixture Proportions and 7-day Strength Properties.

Mixture ID	Plain Concrete		Fiber Reinforced Concrete	
	PCC		FRC	
Material	kg/m ³	lb/yd ³	kg/m ³	lb/yd ³
Water	183	308	183	308
Type I Cement	360	607	360	607
Coarse aggregate	976	1645	976	1645
Fine aggregate	807	1360	807	1360
Synthetic Fibers	---	---	7.2	12.1
Properties	MPa	Psi	MPa	Psi
Compressive Strength (f _c)	28.9	4,192	28.5	4,134
Split Tensile Strength (f _t)	3.5	508	4.4	638

The plain and FRC batches were mixed at approximately the same time. The layered specimen shown in Figure 1 was created by first casting and consolidating the bottom layer (material 2). The top layer (material 1) was then placed into the mold. Consolidation of the top layer (material) included 25mm penetration into the bottom layer (material 2) to ensure a graded interface zone between the two materials. The specimens

were moist cured for 7-days before testing. One day before testing, a notch one third of the specimen depth was cut into each specimen.

TABLE 3. Properties of Synthetic Fibers.

Fiber Type	Synthetic Fiber
Photo	
Material	Polypropylene/ Polyethylene
Cross Section	Rectangular
Length (mm)	40
Thickness (mm)	0.105
Width (mm)	1.4
Aspect Ratio	90
Specific Gravity	0.92
Tensile Capacity (MPa)	620
Modulus of elasticity (GPa)	9.5

The compressive and split-tensile strengths of each mixture were determined without layering the materials in the cylinders (102 mm diameter by 203 mm length). The compressive strength and split-tensile strengths at 7-days are shown in Table 2. The addition of fibers did not affect the compressive strength of the plain concrete, but the higher fiber content mixtures resulted in slightly increased split tensile strength over plain concrete which typically is seen when fiber contents approach 1 percent (11, 15).

TEST RESULTS AND CALCULATION OF FRACTURE PARAMETERS

Two-Parameter Fracture Model (TPFM)

In order to numerically simulate the fracture behavior of the functionally layered concrete specimens, the Two-Parameter Fracture Model (12) was first used to quantify the fracture parameters of the monolithic concrete beam specimens (PCC or FRC). The TPFM idealizes the nonlinear fracture behavior of concrete materials by assuming an effective elastic crack and then employing linear elastic fracture mechanics. The notched TPB specimens seen in Figure 1 were used to derive two fracture parameters. The TPB dimensions were 700 x 150 x 80 mm with an initial notch depth (a_0) of 50 mm. The beam specimen has a ligament depth of $h - a_0$, and therefore:

$$h_1 = h_2 - a_0 \quad (1)$$

to ensure that the effective cross-sectional area under testing is equal in both layers. In the TPB specimen where $h=150$ mm and $a_0=50$ mm, the depth of layer 1 is $h_1=50$ mm and $h_2=100$ mm.

The testing guidelines for the TPFM are specified by RILEM (13). The load (P) and crack-mouth-opening-displacement (CMOD) are recorded. Each TPB specimen was subjected to ten cycles of loading and unloading followed by a final cycle of loading until the beam fractured or the CMOD gauge went out of range. Figure 2 shows the monotonic load-CMOD curve for a plain concrete specimen and also the envelope curve encompassing the load-unload cycles.

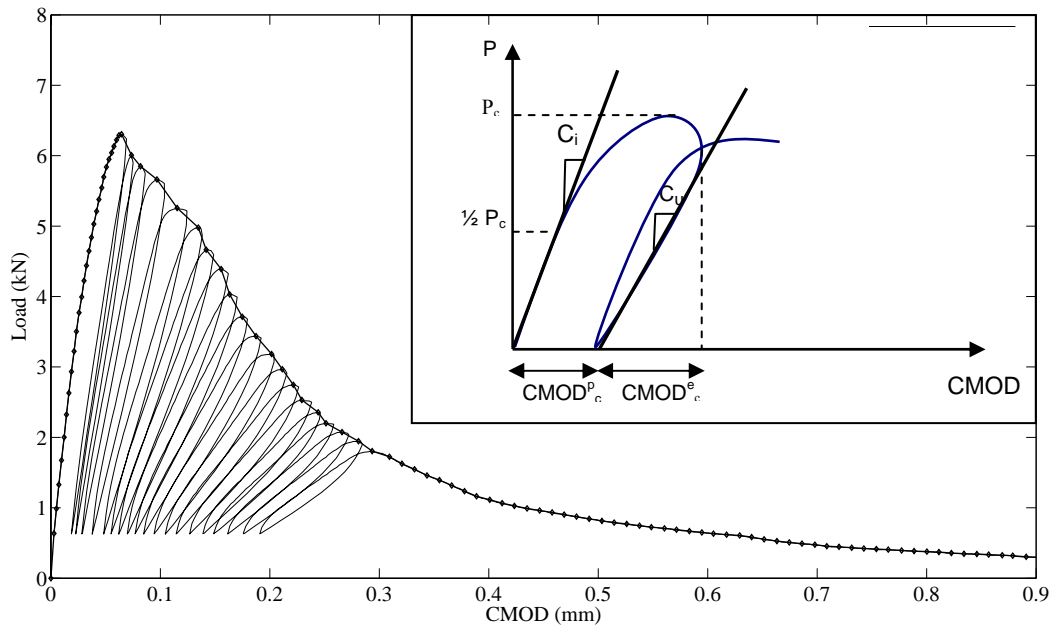


FIGURE 2 Load-CMOD curve for plain concrete specimen with compliance cycles and envelope curve along with definition of loading and unloading compliance (C_i and C_u) from the load (P) versus crack mouth opening displacement (CMOD) plot.

Two fracture parameters, critical stress intensity factor (K_{IC}) and crack tip opening displacement ($CTOD_C$), were calculated from the loading and unloading compliance curves. The loading and unloading compliance values were determined from the first load-unload cycle, as depicted in Figure 2. The loading compliance (C_i) was calculated as the inverse of the slope from zero until the load reached half of the peak load ($\frac{1}{2} P_c$). The specimen was unloaded after the load decreased 5% from peak load. The unloading compliance (C_u) was calculated as the inverse of the slope of the unloading curve from 80 percent of the peak load of the cycle until the minimum load.

The K_{IC} and $CTOD_C$ were calculated by first obtaining the critical effective crack length (a_c) at the peak load. This is completed by equating the modulus of elasticity obtained with the loading and unloading compliance, E_i and E_u , respectively:

$$E_i = \frac{6sa g_2(\alpha_0)}{C_i w^2 t} \quad (2)$$

$$E_u = \frac{6sa_c g_2(\alpha_c)}{C_u w^2 t} \quad (3)$$

where (s) is the span, (w) the depth, (t) the width and (a_0) the initial notch depth of the beam. The variables α_0 , α_c and $g_2(\alpha)$ are the initial notch/depth ratio, critical notch/depth ratio and opening displacement geometric factor for the TPB specimen, respectively.

Once the critical effective elastic crack length, a_c , is computed, then the critical stress intensity factor (K_{IC}) can be calculated from the following:

$$K_{IC} = 3(P_c + 0.5W_0 s / l) \frac{s \sqrt{\pi a_c} g_1(a_c / w)}{2w^2 t} \quad (4)$$

where (P_c) is the peak load, (W_0) is the self-weight of the specimen, l is the length of the specimen and (g_1) is the geometric function for the beam specimen defined as:

$$g_1\left(\frac{a_c}{w}\right) = \frac{1.99 - (a_c / w)(1 - a_c / w)[2.15 - 3.93(a_c / w) + 2.70(a_c / w)^2]}{\sqrt{\pi}[1 + 2(a_c / w)][1 - (a_c / w)]^{3/2}} \quad (5)$$

Finally, the $CTOD_C$ is calculated using:

$$CTOD_c = 6(P_c + 0.5W_0 s / l) * \frac{sa_c g_2(a_c / w)}{E w^2 t} * \left[(1 - (a_c / a_0))^2 + [1.081 - 1.149\left(\frac{a_c}{w}\right)] * [(a_c / a_0) - (a_c / a_0)^2] \right]^{1/2} \quad (6)$$

with $g_2(\alpha)$ given by:

$$g_2(\alpha) = 0.76 - 2.28\alpha + 3.87\alpha^2 - 2.04\alpha^3 + \frac{0.66}{(1 - \alpha)^2} \quad (7)$$

For plane stress, the energy release rate G_f or initial fracture energy is related to K_{IC} and the modulus of elasticity, E , by the following equation:

$$G_f = \frac{K_{IC}^2}{E} \quad (8)$$

Table 4 presents the average P_c , K_{IC} , G_f , a_c and $CTOD_C$ results obtained from TPB tests. The use of fibers did not significantly affect the peak load of the specimens, and subsequently did not significantly change the calculated K_{IC} , G_f , and $CTOD_C$. It can be also seen that the critical crack length is very similar between samples. It is important to notice that these properties are related just to the stage of crack initiation instead of crack propagation, which is why the initial properties did not differ much since the same concrete constituents and proportions were used for both the PCC and FRC specimens.

Table 4. Average Fracture Parameters for TPB Specimens

Top / bottom layer	P_c (kN)	K_{IC} (MPa·m ^{1/2})	$CTOD_c$ (mm)	G_f (N/m)	a_c (mm)	G_{2mm} (N/m)	G_F (N/m)
PCC / PCC	3.710	1.05	0.016	38.1	61.8	119	119
FRC / FRC	3.482	1.03	0.016	36.9	66.5	378	3,409
PCC / FRC	3.714	1.08	0.017	40.3	65.7	249	-
FRC / PCC	3.569	0.96	0.016	35.2	61.6	216	-

Total Fracture Energy (G_F)

The total fracture energy (G_F) was calculated based on a method proposed by Hillerborg (14), which is defined as the ratio between the total energy (W_t), and the concrete fracture area $(w - a_0)t$. The total energy (W_t) is calculated using the sum of the area under the raw load (P_a) vs. CMOD envelope curve (W_r) and $P_w\delta_0$, where P_a is the raw load applied by the testing machine (without considering self-weight), P_w is the equivalent self weight force, and δ_0 is the CMOD displacement corresponding to $P_a=0$ at failure. The raw load versus CMOD for each layered system is shown in Figure 3. The equivalent self weight force is calculated as $P_w=(s/(2l))W_o$, where s is the span, l is the specimen length and W_o is the specimen weight.

The total fracture energy was calculated as:

$$G_F = \frac{W_t}{(w - a_0)t} = \frac{W_r + 2P_w\delta_0}{(w - a_0)t} \quad (9)$$

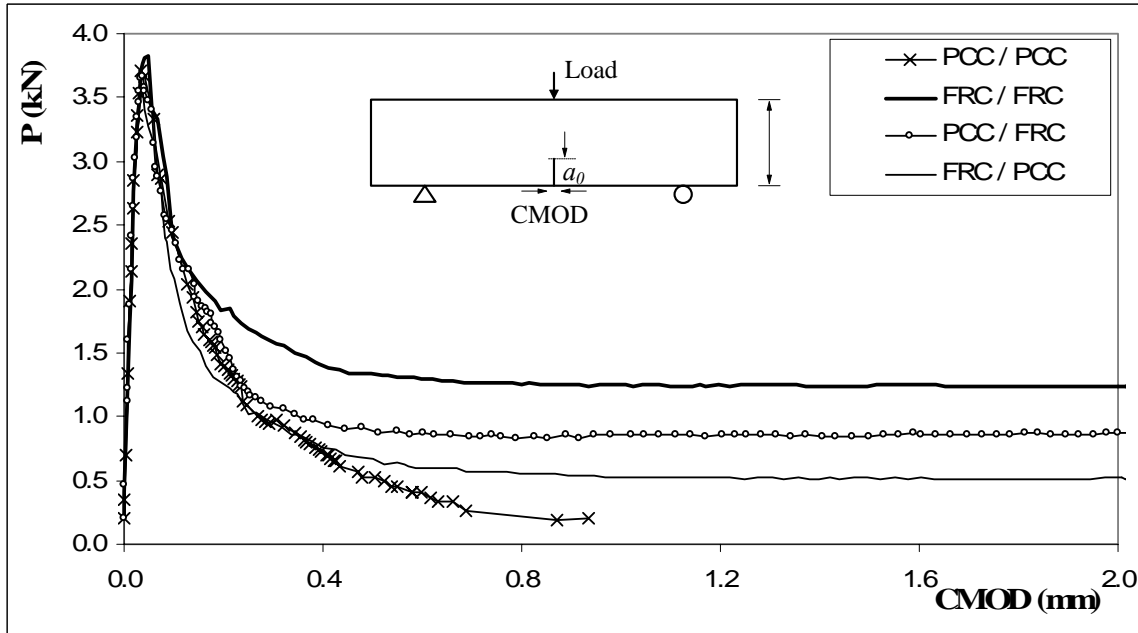


FIGURE 3. Average Load – CMOD envelope curves for TPB specimens with plain, synthetic fiber, and functionally layered concrete.

Due to fibers ability to effectively bridge cracks, the load can remain constant until large values of CMOD, as seen in Figure 4. In order to determine the total fracture energy of the FRC beams and not the fracture energy at any arbitrary opening displacement, additional TPB tests were performed using an LVDT to measure the CMOD until the raw load reached approximately zero, as seen in Figure 4. The area under the envelope curve until failure ($P_a=0$) and a $CMOD_{max}=\delta_0 = 2$ mm were then used to calculate two fracture energy quantities for the FRC, respectively: total fracture energy (G_F) and relative fracture energy (G_{2mm}). The relative fracture energy calculated at 2 mm opening displacement was selected since many CMOD devices have ranges from 2 to 4mm and the maximum crack width desired in fractured concrete slabs is typically between 1 and 2.5 mm.

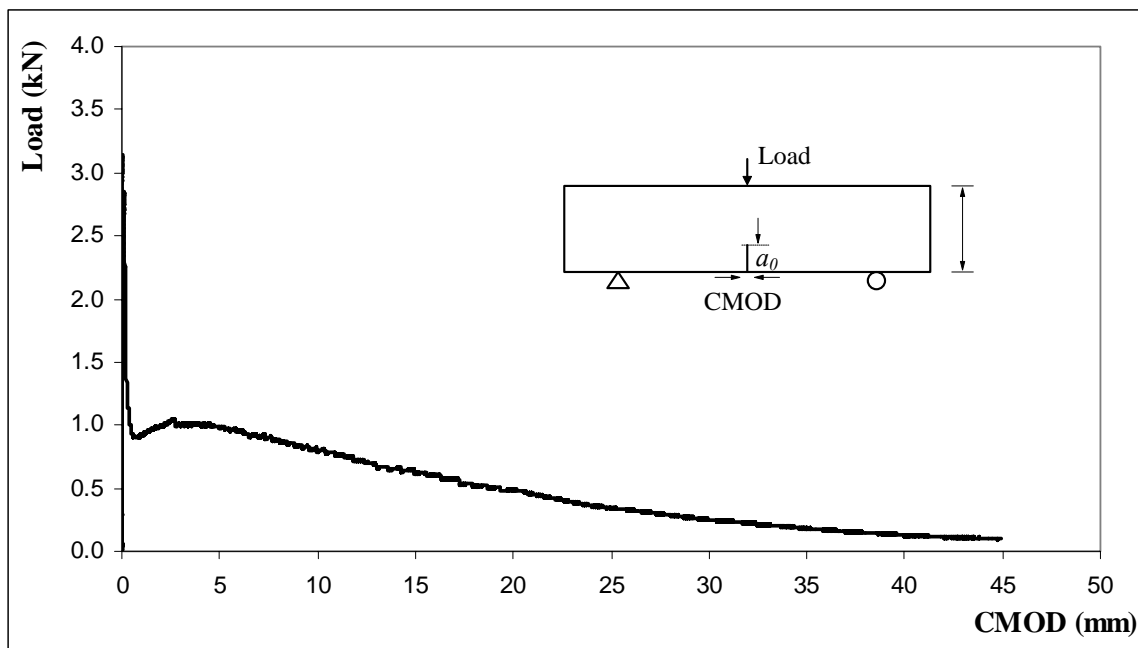


FIGURE 4. Average Load-CMOD envelope curve for TPB specimen with FRC.

Figure 3 does not show a significant difference in peak loads between specimens, with all peaks in a range between 3.48 and 3.71 which is a coefficient of variation of just 6 percent. However, big differences can be seen when comparing the area under the Load-CMOD curves. As shown in Figure 3, the FRC/FRC and PCC/FRC specimens had significantly better fracture resistance compared to plain concrete (PCC/PCC). The FRC/PCC specimens still behaved better than plain concrete, but had a lower residual strength compared with the other FRC specimens. Table 4 shows that fibers dispersed throughout the full-depth of the beam increased the G_{2mm} by 218 percent over plain concrete. Specimens with PCC on top and FRC on the bottom (PCC/FRC) had a higher G_{2mm} than samples with FRC on top and PCC on the bottom (FRC/ PCC). The addition of fibers to the bottom or top layer improved G_{2mm} by 109 and 82 percent in comparison to PCC/PCC, respectively.

NUMERICAL MODELING FOR NONLINEAR FRACTURE PROCESS ZONE

General Description

In order to numerically predict the fracture behavior of the FGCM shown in Figure 3, a finite element-based model which can describe the nonlinear fracture process zone present in concrete materials is required. This objective is achieved by first defining a mesh with bulk elements that represent the material at the top and bottom layer, as shown in Figure 5(a). This mesh is refined close to the crack tip and cohesive elements are inserted in the expected crack path. These cohesive elements, shown in Figure 5(b), require a softening model to represent the fracture behavior of the material located in the respective layers, i.e. plain concrete and FRC. This numerical model must be able to predict the constitutive behavior of PCC/PCC and FRC/FRC specimens as well as the FGCM samples, PCC/FRC and FRC/PCC.

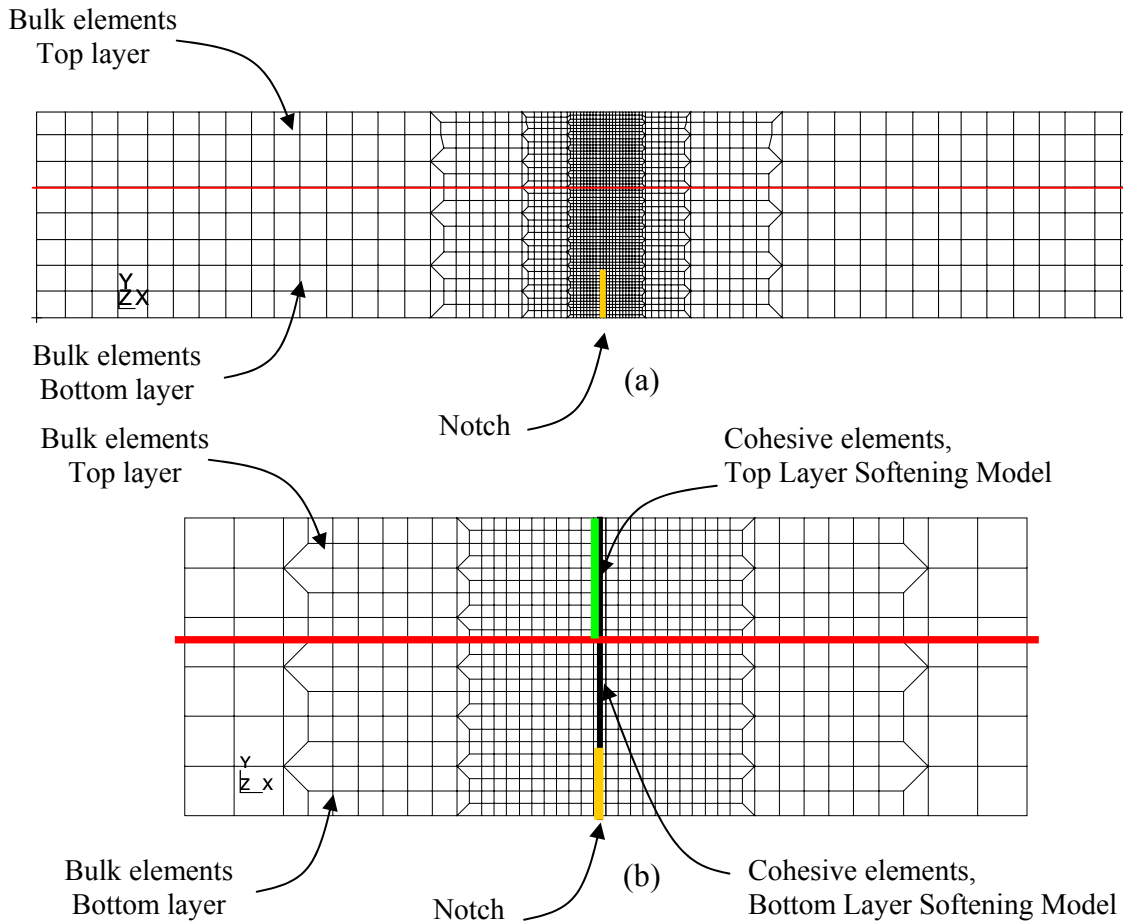


FIGURE 5. (a) Finite element mesh; and (b) zoom in of the mesh along the cohesive element region.

Softening Model for Plain Concrete

Under monotonically increasing load, progressive cracking in plain concrete can be idealized as a zone of distributed micro-cracks, a bridging zone and a traction free macro-crack zone, as shown in Figure 6(a). Micro-cracks initiate ahead of the bridging zone before the applied stress reaches the material's tensile strength (f'_t). When the stress reaches the tensile strength, micro-cracks grow and coalesce, which produces the bridging zone, also called the nonlinear fracture process zone. This zone results from the crack branching and interlocking as a result of the weak interface between the aggregates and cement matrix (16, 17). The nonlinear process zone connects the micro-crack and a traction free macro-crack zones. When a crack opening width is greater than a certain value, called the final crack opening width (w_f), a macroscopic crack appears which cannot transfer traction along its surfaces anymore.

The nonlinear fracture process zone for concrete is best characterized by the cohesive zone model (CZM) (18), as depicted in Figure 6(a). The softening curve in the CZM is physically-defined by four experimental fracture parameters (19): tensile strength, initial fracture energy (G_f), total fracture energy (G_F) and critical crack tip opening displacement ($CTOD_c$). The initial fracture energy defines the horizontal axis intercept (w_l) of the initial softening slope (20), expressed as:

$$w_l = \frac{2G_f}{f'_t}. \quad (10)$$

The kink point of the crack opening width (w_k) is hypothesized (19) as

$$w_k = CTOD_c, \quad (11)$$

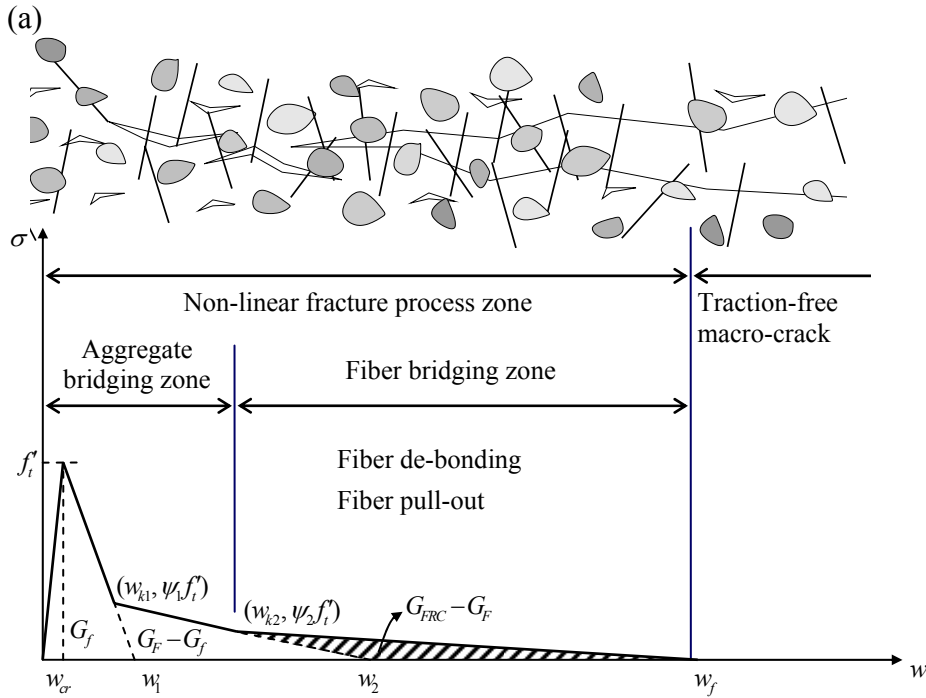
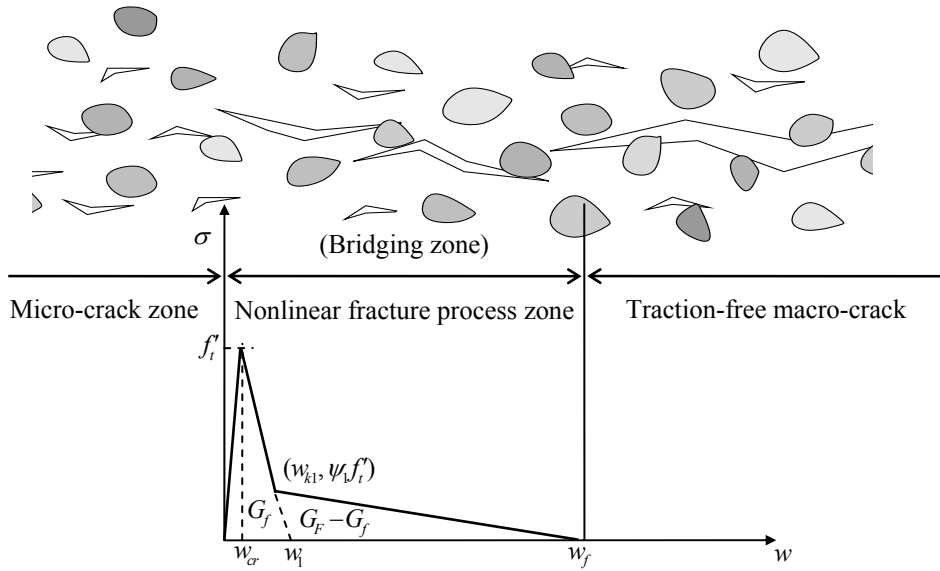
which results in the determination of the stress ratio (ψ) at the kink point, i.e.

$$\psi = 1 - \frac{CTOD_c f'_t}{2G_f}. \quad (12)$$

The final crack opening width is calculated as

$$w_f = \frac{2}{\psi f'_t} [G_F - (1 - \psi)G_f], \quad (13)$$

which is obtained by equating the total fracture energy with the area under the softening model for plain concrete (14).



(b)
FIGURE 6. Fracture mechanisms and experimental fracture parameter based softening model for (a) plain concrete and (b) FRC.

Softening Model for FRC

Fracture mechanisms of FRC are different from those of plain concrete due to the effect fibers have on the nonlinear fracture process zone (17), as shown in Figure 6(b). Although fibers do not generally influence the tensile strength or early post-peak behavior at low volume fractions, fibers do increase the total fracture energy of plain concrete, which results in the observed high post-peak load behaviors (15). These same features can be observed in the softening curves shown in Figures 3 and 4. As a result,

the nonlinear fracture process zone for FRC is further divided into the aggregate bridging zone and the fiber bridging zone, as shown in the model diagrammed in Figure 6(b). The aggregate bridging zone is represented by the same softening model for plain concrete. The fiber bridging zone is characterized by a linear descending slope (21), which characterizes the fiber de-bonding and pull-out mechanisms.

The softening model for FRC is determined by the total fracture energy (G_{FRC}) and w_f of FRC and four experimental fracture parameters (f'_t , G_f , G_F , $CTOD_c$) of plain concrete. G_{FRC} is the fracture energy from the full load-CMOD curve as shown in Figure 4. Since fibers have limited influence on the aggregate bridging zone, the first kink point (w_{k1} , $\psi_1 f'_t$) in the softening model for FRC is the same as the kink point (w_k , $\psi f'_t$) in the model for plain concrete. The second kink point (w_{k2} , $\psi_2 f'_t$) is evaluated with the total fracture energy of FRC (G_{FRC}) and the assumption of w_f , expressed as

$$\psi_2 = \frac{2(G_{FRC} - G_F)}{f'_t (w_f - w_2)}, \quad (14)$$

and

$$w_{k2} = w_2 - \frac{\psi_2}{\psi_1} (w_1 - w_{k1}). \quad (15)$$

In this study, the final crack opening width is estimated as a quarter of the fiber length, which corresponds to the averaged pull-out length for randomly distributed fibers reported in the literature (22-24). On going research is being conducted to provide a basis for the w_f estimation given a specific fiber type and concrete matrix.

Comparison between Experimental and Numerical Results

The bulk FEM model with the cohesive zone models (CZM) proposed for plain and fiber reinforced concrete were implemented into the commercial finite element program ABAQUS as a user element subroutine. Based on previous convergence studies (25), the size of the cohesive element was selected to be 1 mm. Figure 6 illustrates the correspondence between the experimental fracture results and the numerical simulations for the different combinations of concrete layers. The cohesive zone models based on the measured fracture parameters of the plain concrete and FRC were successfully able to represent the fracture behavior of not only plain and FRC concrete specimens but also FGCM specimens (FRC/PCC and PCC/FRC).

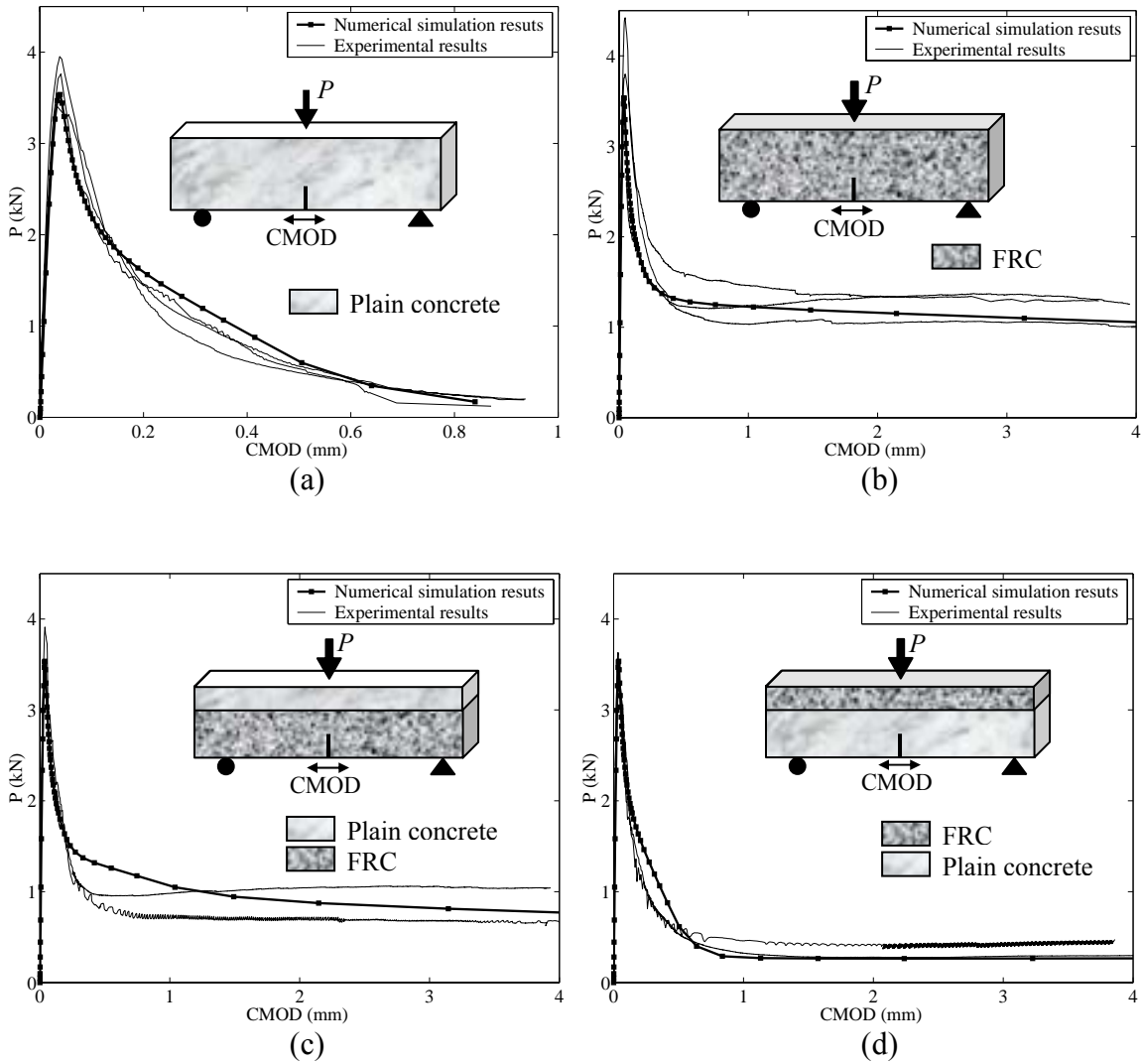


FIGURE 7. Comparison between experimental and numerical simulation results for (a) plain concrete (PCC/PCC), (b) fiber reinforced concrete (FRC/FRC), (c) FRC layer at the bottom (PCC/FRC), and (d) FRC layer at the top (FRC/PCC).

Figure 8 shows that the nonlinear cohesive zone models for FRC and plain concrete specimens are shown to be similar to the actual experimental results. Figure 8 also demonstrates that the FGCM fracture behavior can be correctly predicted as seen in the case where the FRC layer at the notch location (PCC/FRC) results in a higher post-peak response than when the FRC layer is cast in the top part of the specimen (FRC/PCC).

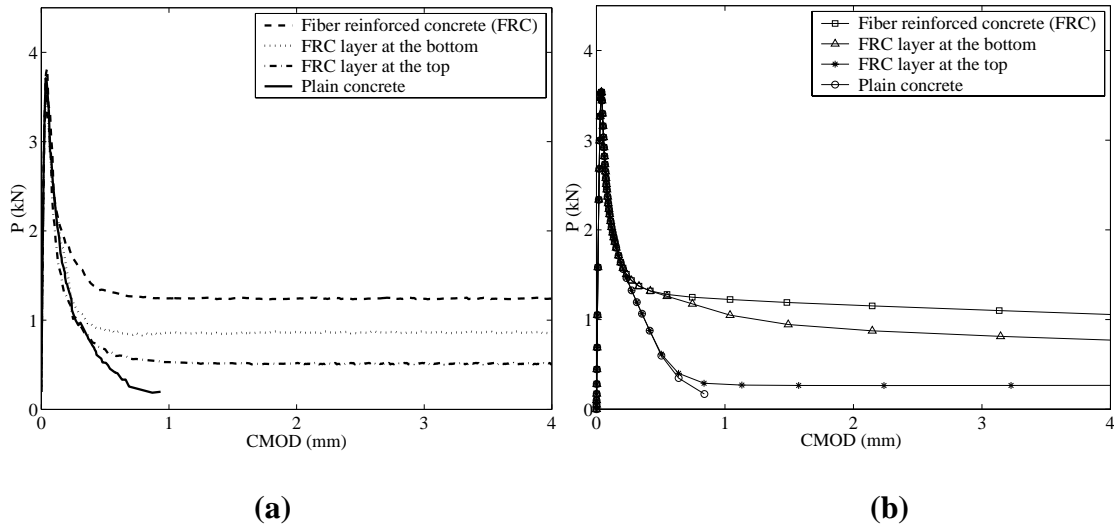


FIGURE 8. Comparison between (a) experimental results and (b) numerical simulation of TPB specimens.

Effect of layering on specimen fracture behavior

When using synthetic fibers, the specimens with FRC on the bottom had higher fracture energy (G_{2mm}) relative to the specimen with FRC on the top. This result happens because the synthetic fibers modulus is closer to the concrete matrix modulus allowing for effective crack bridging behind the crack front. Synthetic fibers near the top of specimen were not able to dissipate as much energy due to the lower amount of fiber bridging behind the crack front.

This preliminary testing suggests the use of FGCM for rigid pavement can be used to optimize the materials and concrete pavement fracture behavior. The accompanying numerical analysis based on the CZM formulation was also able to reasonable predict the fracture behavior of the FGCM. This numerical analysis tool is essential to quantify the fracture behavior of various concrete materials, thicknesses, and placements within the surface concrete layer for future FGCM systems (26), since excessive testing would be required to quantify the fracture behavior of all fiber types, volume fractions, layer depths, and concrete mixture designs.

The proof of concept testing and analysis presented has shown concrete material properties and placement in a structure can affect the fracture behavior of the system. Improvements in the overall fracture behavior of concrete pavements can be realized and result in thinner slabs and fewer joints. Furthermore, FGCM enables utilization of lower quality construction materials, such as recycled concrete, in certain regions of the slab without sacrificing overall pavement performance.

CONCLUSION

The application of functional graded (or layered) concrete materials (FGCM) for rigid pavement has shown promising results based on fracture testing and numerical modeling. As expected, all concrete specimens that used fibers showed an improved residual strength or softening behavior over plain concrete. The initial fracture energy and critical crack tip opening displacement did not differentiate the differences in fracture behavior of the plain, fiber reinforced, and functionally layered concrete. The total fracture energy (G_F) or the fracture energy up to 2mm opening displacement (G_{2mm}) were the key indicators quantifying how the fiber reinforced and functional graded concrete improved the cracking resistance of plain concrete specimens. The improvement in the concrete G_{2mm} was closely related to the depth and position of the fibrous concrete layer. The FGCM with fiber reinforced concrete was more fracture resistant (increased G_{2mm}) when the fibers were placed closest to the notch and slightly less efficient when the fibers were placed near the top of the specimen. The fiber bridging mechanism behind the crack front was the primary mechanism resulting in a higher residual load capacity.

An integrated approach involving testing and modeling was successfully implemented in this research investigation. A finite element-based cohesive zone model (CZM) was developed to predict the softening behavior of the FGCM systems based on the individual concrete material fracture properties. The numerical simulation of FGCM, based on the measured plain and fiber reinforced concrete fracture parameters, was able to match the experimental results of the various combinations of plain concrete and FRC. The CZM prediction of the experimental results were very promising and demonstrate the viability of FGCM and the CZM for characterizing and designing layered concrete pavement systems.

ACKNOWLEDGMENTS

The authors would like to acknowledge support through the Center of Excellence for Airport Technology (CEAT) provided by the O'Hare Modernization Plan (OMP) and the City of Chicago for their financial support in this study. The information presented in this paper is the sole opinion of the authors and does not reflect the views of the sponsoring agencies.

REFERENCES

1. Hirano T., J. Teraki, and T. Yamada. On the Design of Functionally Gradient Materials. In *Proceedings of the First International Symposium on Functionally Gradient Materials*. Editors Ymanouchi M., M. Koizumi, T. Hirai, and L. Shiota, Sendai, Japan, 1990, pp. 5-10.
2. Hirai T. Functionally Gradient Materials and Nanocomposites. In *Proceedings of the Second International Symposium on Functionally Gradient Materials*. Editors Holt J.B., M. Koizumi, T. Hirai, and Z.A. Munir. *The American*

- Ceramic Society: Ceramic Transactions*, Vol. 34, Westerville, Ohio; 1993, pp. 11-20.
3. Miyamoto Y., W.A. Kaysser, B.H. Rabin, A. Kawasaki, and R.G. Ford. *Functionally Graded Materials: Design, Processing and Applications*. Kluwer Academic Publishers, Dordrecht, 1999.
 4. Paulino, G.H., Z.-H. Jin, and R.H. Dodds. Failure of Functionally Graded Materials. In *Comprehensive Structural Integrity*. Editors Karihaloo and Knauss, Vol. 2, Chapter 13, Elsevier, Amsterdam, 2003, pp. 607-644.
 5. Ilschner, B. Technical Resume of the 5th International Symposium on Functionally Graded Materials. *Materials Science Forum* Vol. 308-311, 1999, pp. 3-10.
 6. Darter, M.I. *Report on the 1992 U.S. Tour of European Concrete Highways*. Federal Highway Administration, 1992, pp. 124.
 7. Smiley, D.L. *First Year Performance of the European Concrete Pavement on Northbound I-75 – Detroit, Michigan*. Michigan Department of Transportation, 1995, pp. 22.
 8. Cable, J. K. and D.P. Frentress. *Two-Lift Portland Cement Concrete Pavements to Meet Public Needs*. Federal Highway Administration Technical Report, 2004.
 9. Ravindrarajah, R. S. and C.T. Tam. Flexural Strength of Steel Fibre Reinforced Concrete Beams. *International Journal of Cement Composites and Lightweight Concrete*, Vol. 6, No. 4, 1984, pp. 273-278.
 10. Zhang, J. and V.C. Li. Monotonic and fatigue performance in bending of fiber-reinforced engineered cementitious composite in overlay system. *Cement and Concrete Research*, Vol. 32, 2002, pp. 415-423.
 11. Balaguru, P. and S.P. Shah. *Fiber Reinforced Cement Composites*. McGraw-Hill, 1992.
 12. Jenq, Y. and S.P. Shah. Two Parameter Model for Concrete. *Journal of Engineering Mechanics*, Vol. 111, No. 10, 1985, pp. 1227-1241.
 13. RILEM Committee on Fracture Mechanics of Concrete-Test Methods. Determination of the Fracture Parameters (K_{SIC} and $CTOD_c$) of Plain Concrete Using Three-Point Bend Tests. *Materials and Structures*, Vol. 23, 1990, pp. 457-760.
 14. Hillerborg, A. The Theoretical Basis of a Method to Determine the Fracture Energy G_F of Concrete. *Material and Structures, RILEM*, Vol. 16, 1985, pp. 291-296.

15. Shah, S.P. Do fibers increase the tensile strength of cement-based matrixes? *ACI Materials Journal*, Vol. 88, No. 6, 1991, pp. 595-602.
16. Anderson, T.L. *Fracture Mechanics: Fundamentals and Applications*. CRC Press, Boca Raton, 1995.
17. Van Mier, J.G.M. *Fracture Processes of Concrete: Assessment of Material Parameters for Fracture Models*. CRC Press, Boca Raton, 1996.
18. Roesler, J.R., G.H. Paulino, K. Park, and C. Gaedicke. Concrete fracture prediction using bilinear softening. *Cement and Concrete Composites*, under review 2006.
19. Park, K., G.H. Paulino, and J.R. Roesler. Determination of the kink point in the bilinear softening model for concrete. *ASCE Journal of Materials in Civil Engineering*, under review, 2006.
20. Bazant, Z.P. and M.T. Kazemi. Determination of fracture energy, process zone length and brittleness number from size effect, with application to rock and concrete. *International Journal of Fracture*, Vol. 44, 1990, pp. 111-131.
21. Park, K., G.H. Paulino, A. Bordelon, and J.R. Roesler. Experimental based softening model for fiber reinforced concrete. (To be submitted for journal publication), 2006.
22. Gopalaratnam, V.S. and S.P. Shah. Tensile failure of steel fiber-reinforced mortar. *ASCE Journal of Engineering Mechanics*, Vol. 113, No. 5, 1987, pp. 635-652.
23. Fu, S.Y. and B. Lauke. Effects of fiber length and fiber orientation distributions on the tensile strength of short-fiber-reinforced polymers. *Composites Science and Technology*, Vol. 56, No. 10, 1996, pp. 1179-1190.
24. Lok, T.S. and J.S. Pei. Flexural behavior of steel fiber reinforced concrete. *Journal of Materials in Civil Engineering*, Vol. 10, No. 2, 1998, pp. 86-97.
25. Song SH, Paulino GH, Buttlar WG. Simulation of crack propagation in asphalt concrete using a cohesive zone model. *ASCE Journal of Engineering Mechanics*. Vol.132, 11, 2006, pp.1215-1223.
26. Altoubat, Salah A., J.R. Roesler, D. A. Lange, and K.-A. Rieder. Simplified Method for Concrete Pavement Design with Discrete Structural Fibers. *Construction and Building Materials*, 2006, (in press).